Available online at www.sciencedirect.com
ScienceDirect
Journal of Power Sources 164 (2007) 49–55
JOURNAL OF POWER SOURCES
www.elsevier.com/locate/jpowsour

# Preparation of three-dimensional composite of poly(*N*-acetylaniline) nanorods/platinum nanoclusters and electrocatalytic oxidation of methanol

Chunming Jiang, Xiangqin Lin *

*Department of Chemistry, University of Science and Technology of China, Hefei 230026, PR China*

Received 12 September 2006; received in revised form 8 October 2006; accepted 9 October 2006
Available online 22 November 2006

**Abstract**

Preparation of nanocomposites of precious metal/conducting polymer is interested in studies of nanoscience and technology and in the fields of fuel cells applications. In this work, a 3D matrix of the novel nanocomposite on a glassy carbon electrode (GCE) was presented, which is consisted of nanorods of poly(*N*-acetylaniline) (nr-PAANI) and embedded platinum nanoclusters (nc-Pt). The nc-Pt/nr-PAANI nanocomposite was electrochemically in situ deposited in two steps: first, the nr-PAANI matrix was deposited on GCE by potential cycling between −0.2 and 1.0 V versus SCE; then, the nc-Pt was deposited on the nr-PAANI modified electrode by potential cycling between −0.2 and 0.8 V. The unique 3D structure of the nr-PAANI, nc-Pt and nc-Pt/nr-PAANI was characterized by X-ray photoelectron spectroscopy (XPS), field emission scanning electron microscope (FE-SEM), X-ray diffraction (XRD), UV–visible spectroscopy (UV–vis) and cyclic voltammetry techniques. The nanocomposite acted as a high efficient catalyst with enhanced anti-poisoning ability for the electrochemical oxidation of methanol in 0.5 M $H_2SO_4$. Based on our observations, a mechanism for the synergic effect of the poly(*N*-acetylaniline) (PAANI) in the nanocomposite was proposed.


*Keywords:* Nanostructure; Composite; Poly(*N*-acetylaniline); Methanol; Catalytic oxidation

## 1. Introduction

Electrochemical catalytic oxidation of methanol has been extensively studied for its possible usage as a fuel in the direct methanol fuel cells (DMFC) [1]. Development of efficient fuel cells is greatly contributed form the catalyst design [2,3]. Major criteria for the anode catalysts are high electrocatalytic activity and low poisoning in the methanol oxidation. The poisoning effect is mainly considered as the adsorption of carboxyl intermediates generated from the oxidation [4]. In the recent years, beside metal/metal composite, metal or metal alloy/polymer composite systems have been investigated for promoting the catalytic activity and reducing the poisoning effect. For dispersion of metal particles in a polymer matrix, electrochemical deposition methods have been widely used. Especially for fabrication of the matrix of conducting polymers, such as polyaniline [5–12], polypyrrole [13–17], polythiophene [18] and polyphenylenediamine [19], electrochemical deposition methods have shown advantages of simple, in situ and high dispersion. The high dispersion leads to high ratio of surface area/metal loading, which is usually considered as the major parameter characterizing the efficiency of the catalyst.

Synergistic effects between the metal particles, such as Pt, Pd, Ru, Cr, Co, Sn and related alloys, and the incorporated polymeric matrix have been observed and very much interested by many researchers. However, detailed mechanism for explanation of the effect in promoting the electrocatalytic activity and reducing the poisoning in comparison with individually modified electrodes is still not clear.

It is also of interest to extend such studies to other polymers, which might be suitable as the host material of the catalyst nanoparticles. One of substituted polyaniline conducting polymers, poly(*N*-acetylaniline) (PAANI), has been extensively investigated in the fields of biosensors fabrication in our research group [20–22]. In this paper, we try to investigate the composite

* Corresponding author. Tel.: +86 551 3606646; fax: +86 551 3601592.
*E-mail address:* xqlin@ustc.edu.cn (X. Lin).

0378-7753/$ – see front matter © 2006 Elsevier B.V. All rights reserved.
doi:10.1016/j.jpowsour.2006.10.057

effect of Pt nanoparticles and PAANI matrix for electrocatalytic oxidation of methanol. Under very carefully selected experimental conditions, a novel 3D PAANI nanorod (nr-PAANI) matrix and a unique 3D nanocomposite of Pt nanoclusters (nc-Pt) embedded nr-PAANI (nc-Pt/nr-PAANI) were prepared. Furthermore, we found that the nc-Pt/nr-PAANI nanocomposite modified layer can act as an efficient catalyst for the oxidation of methanol with reduced poisoning effect. A reaction mechanism for the formation of the nanostructures and the synergistic effect of the composite is proposed.

## 2. Experimental

### 2.1. Instruments and reagents

*N*-acetylaniline was purchased from the Changping-Kuangying Chemical Reagent of Beijing (Beijing, China) and used after recrystallization from ethanol. $H_2PtCl_6$, $HClO_4$, $CH_3OH$, $H_2SO_4$, $CH_2O$, $C_2H_6O$ and dimethyl sulfoxide (DMSO) were obtained from Chemical Reagent Company of Shanghai (Shanghai, China). These chemicals were analytical grade and used as received without further purification. Doubly distilled water and high purity nitrogen were used.

Electrochemical experiments were conducted on CHI832 electrochemistry workstation (Chen-Hua, Shanghai, China) with a three-electrode system consisted of a testing electrode, a platinum wire auxiliary electrode and a saturated calomel reference electrode (SCE). Glassy carbon disk electrodes (GCE, Ø = 4.0 mm, formal surface area = 0.126 $cm^2$) (Lan-Like HCET Company, Tianjin, China) were used as the basal electrodes for the fabrication. All potentials, in the paper were reported versus SCE.

Experiments were carried out at room temperature. $N_2$ bubbling was used for solution deaeration and maintaining the atmosphere in the cell through out experiment.

Measurements of X-ray photoelectron spectroscopy (XPS) were carried out on ESCALAB MK2 photoelectron spectrometer (VG, UK) equipped with the Mg Kα X-ray radiation as the source for excitation at a pressure of less than $10^{-9}$ Torr in the chamber.

Images of field emission scanning electron microscope (FE-SEM) were obtained on a Sirion-200 field emission scanning electron microanalyser (FEI, Japan).

Patterns of X-ray diffraction (XRD) were recorded on MXPAHF rotating anode X-ray diffract meter (Japan) with a Mo radiation source (λ = 0.70930 Å) at a tube current of 100 mA and a tube voltage of 50 kV.

UV–visible spectroscopy (UV–vis) was performed using a 1 cm path length quartz cuvette and pure DMSO as the reference on UV-2401 (Shimadzu, Japan) spectrophotometer.

### 2.2. Preparation of the electrodes

The basal GCE was first polished by sand papers to a mirror finish. After cleanness, the GCE was dipped in 1.0 M $HClO_4$ solution containing 5.0 mM *N*-acetylaniline for electropolymerization by potential cycling between −0.2 and 1.0 V for 15 cycles at a scan rate of 50 mV $s^{-1}$. The electrode obtained was denoted as PAANI/GCE.

The PAANI/GCE was soaked in 0.5 M $H_2SO_4$ + 4.0 mM $H_2PtCl_6$ solution for 30 min, and then a potential cycling at 50 mV $s^{-1}$ between −0.2 and 0.8 V was performed for electrodeposition of platinum. The amount of Pt deposition, the Pt loading, on the electrode surface was controlled by both the pre-adsorption process and the number of the potential cycling. Changes on the cycle number, the potential window and the scan rate of potential cycling could significantly change the property of the fabricated electrode. The electrode obtained was denoted as Pt/PAANI/GCE. The Pt loading was estimated from the charge difference between the CV curves of the PAANI/GCE before and after Pt deposition, assuming that the charging current of the electrode remains constant and the redox efficiency of $Pt^{4+}/Pt^0$ transition is 100% [12].

A nano-Pt deposited GCE was also prepared under the same deposition conditions for comparison, which is denoted as Pt/GCE.

## 3. Results and discussion

### 3.1. Electrochemical deposition of PAANI and Pt

Cyclic voltammetry (CV) was used for electrochemical polymerization and in situ deposition of PAANI film on the basal GCE. CV technique can offer not only the possibilities of controlling the deposited amount and dispersion homogeneity but also the structure of the deposited substances on the electrode surface [23]. According to the result of previous investigation [22], a potential cycling between −0.2 and 1.0 V with a scan rate of 50 mV $s^{-1}$ in 1.0 M $HClO_4$ solution containing 0.1 M *N*-acetylaniline was used for the PAANI deposition. Under these conditions, a well behaved multi-cycle CV curve was recorded during the in situ polymerization and deposition processes, as shown in Fig. 1A. We can see from this figure that the electrooxidation of the *N*-acetylaniline monomer started at about 0.9 V in the first cycle, which generated the initial layer of the PAANI, then three redox couples appeared at $E_m$ about 0.14 (I), 0.50 (II) and 0.75 V (III) and grew up from circle to circle, indicating a conductive polymeric film was depositing onto the electrode surface, forming PAANI/GCE. The steps I and III can be attributed to the oxidation of the phenylene-amine units to the cation radicals and the subsequent oxidation to the radical dications, respectively. The step II is associated with the redox reaction of the degradation product containing aromatic quinonoid groups [24]. For obtaining a suitable surface loading, 15 circles of potential cycling at a scan rate 50 mV $s^{-1}$ was selected for the preparation.

It is known that the formation of $(PtO)_{ads}$ typically observed around 0.1 V and the formation of $(PtH)_{ads}$ observed at potentials lower than 0 V in the reduction of either $PtCl_4^{2-}$ or $PtCl_6^{2-}$ in acidic solutions using CV. Instead of electrolysis at negative potentials [25], a multi-cycle potential cycling was used for the nano-Pt deposition between −0.2 and 0.8 V in this work, forming Pt/GCE. The deposition of Pt on the PAANI/GCE was further conducted in 0.5 M $H_2SO_4$ solution containing $H_2PtCl_6$

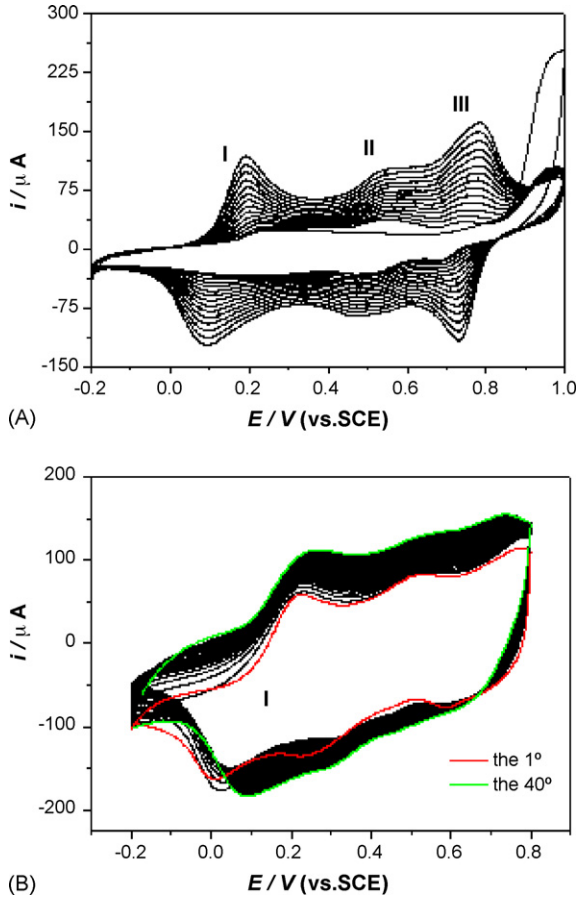


Fig. 1. Multi-cycle CVs: (A) at GCE in 0.1 M *N*-acetylaniline + 1.0 M $HClO_4$; (B) at PAANI/GCE in 0.5 M $H_2SO_4$ + 4.0 mM $H_2PtCl_6$. Scan rate: 50 mV $s^{-1}$.

in the potential window −0.2 to 0.8 V for 40 cycles, as shown in Fig. 1B. However, without appearance of adsorption–desorption waves of hydrogen, which is the criteria to confirm an efficient deposition of Pt/PAANI composite since higher amount of Pt loading could generate the hydrogen waves due to the formation of Pt bulky plates. At the same time, no apparent redox peak concerned to the platinum species can also be found at this potential window. This phenomenon is caused by the initial dipping of the PAANI/GCE in $H_2PtCl_6$ solution inducing the spontaneous reduction of Pt(IV) into the polymer, which significantly reduces the proton and anion doping of the composite material as also demonstrated in Fig. 1B. This implies that the nc-Pt physically blocks the uptake of protons at nitrogen heteroatoms and suggests that the reduction is not necessarily an internal process but rather, a surface process. Recent studies have also shown that Pt(IV) reduction is more favorable at Pt(0) in comparison to the conductive polymer [26,27]. On the other hand, some changes on the shape of PAANI redox peaks were observed during the potential cycling. Compared with the first cycle, the CV curve of the 40th cycle is obviously fatter, which could be simply attributed to an increase of effective surface area of the electrode, resulting from the Pt deposition. Although the steps II and III became slur, the middle potential of step I shifted to the positive direction by 40 mV after 40 cycles scan. The potential shift might indicate

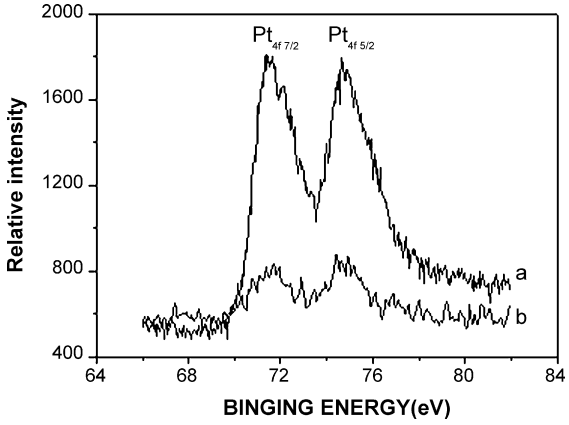


Fig. 2. The XPS of the Pt/PAANI/GCE etched by argon sputters for 0 min (a) and 10 min (b).

a stabilization of the polymer in neutral form due to the Pt deposition.

### 3.2. XPS characterization

The prepared Pt/PAANI/GCE was characterized by XPS, as shown in Fig. 2. For better understanding of the Pt distribution in the polymer matrix, the electrode surface was etched by argon sputters at 3 kV for 0 min (a) and 10 min (b) under vacuum for layered analyses. The curves (a and b) both showed two peaks at 71.4 and 74.6 eV, corresponding to the Pt $4f_{7/2}$ and Pt $4f_{5/2}$ bands, respectively, demonstrating the presence of Pt(0).

### 3.3. SEM morphology and XRD patterns

The FE-SEM images were obtained for the prepared PAANI/GCE and the Pt/PAANI/GCE, as shown in Fig. 3. As seen in Fig. 3A, the porous matrix of PAANI was constructed by short nanorods of 30–40 nm diameter and about 500 nm length, big vertical holes of about 300–500 nm were existed in the stack. This is obviously a result of one-dimensional in situ growth of the conducting polymer, generating one-dimensional conductor of PAANI. To the best of our knowledge, the PAANI nanorods prepared without using any template has never been reported in the literature. Fig. 3B shows a typical image of the nr-PAANI matrix at 38 μg $cm^{-2}$ Pt loadings. As seen from the figure, the PAANI nanorods looked as if they were completely covered by spherical Pt nanoparticles of 60–130 nm size, forming string-of-beads like structure. However, looking carefully, we found that the Pt nanoparticles were actually coated by a layer of amorphous substance, although the layer was almost transparent under the SEM conditions. Obviously, the amorphous substance was the PAANI polymeric chains from the nanorods. On the other words, the large amount of Pt nanoparticles were accumulated in the nanorods, in contrast, few particles were formed directly on the bare GCE.

The XRD pattern of the Pt/PAANI composite is shown in Fig. 4. Three major peaks at 18.1°, 20.7° and 29.9° in the range 5–40° were observed, which can be assigned to the diffraction from (1 1 1), (2 0 0), (2 2 0) and (3 1 1) planes of the face-centered

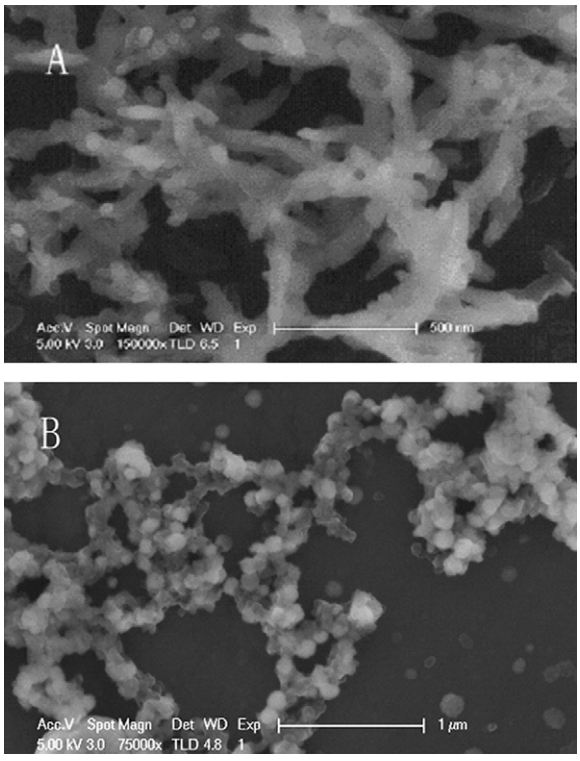


Fig. 3. FE-SEM images of the PAANI/GCE (A) and the Pt/PAANI/GCE with 38.0 μg cm$^{-2}$ Pt loading (B).

cubic lattice of Pt(0), respectively. Thus, the particle size of the Pt can be calculated according to Scherrer's equation [28], $\beta = \kappa\lambda/D\cos\theta$, where $\lambda$ is the X-ray wavelength, $\kappa$ the shape factor (0.89), $\beta$ the average diameter of the particles, $\theta$ the Bragg angle in degree and $D$ is the full-width half-maximum of respective diffraction peak. Based on the reflection peak at $2\theta$ of 18.1°, an averaged diameter of the Pt particles was calculated as 8.5 nm. Hence, the deposited Pt nanoparticles of about 100 nm size were evidently clusters of nano-Pt crystalline (nc-Pt) of 8.5 nm in average size. The nanocluster structure of the deposited Pt can be expected to have higher catalytic activity, which should be not only benefited from its smaller size providing larger surface area/amount of loading, but also from the

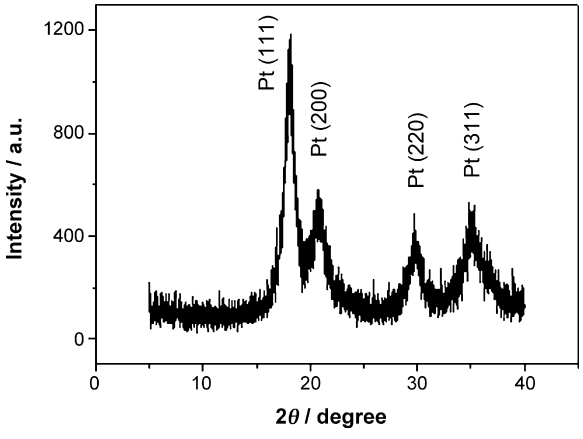


Fig. 4. XRD pattern of the Pt/PAANI composite.

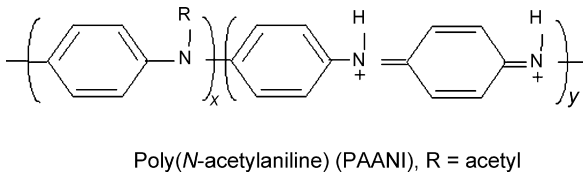


Poly(*N*-acetylaniline) (PAANI), R = acetyl

Scheme 1. Diagram of the structure of poly(*N*-acetylaniline) (PAANI).

cluster structures. Similar sized Pt nanoclusters have been prepared in our group recently [23,29]. By adjusting the parameters of potential cycling, the size of the nanocrystalline and the size of clusters can be easily controlled for obtaining good electrochemical behavior for methanol oxidation.

Unlike the metal nanoparticles embedded in bulky polymeric matrix, the nanostructures and nanodimensions cannot be clearly seen [30], this 3D structure of the nc-Pt embedded nr-PAANI nanocomposite is unique. The feature of the structure is schematically shown in Scheme 1. It is mentioned that the soaking of PAANI/GCE all but ensures that the Pt(0) exists in the PANNI nanorods prior to potential cycling. The Pt(0) centers embedded in the nanorods could further grow up, supplied by the reduction of $PtCl_6^{2-}$ diffusion from the bulk solution when cyclic scanning.

### 3.4. Spectral characterization

For demonstration of the interactions between PAANI and Pt species, UV–vis spectra were obtained for PAANI film before and after dipping in $PtCl_6^{2-}$ solutions. The result is shown in Fig. 5. The films were scraped from the electrodes and dissolved in DMSO for spectral determination. The PAANI showed two absorption peaks at 330 and 650 nm, which correspond to the $\pi$–$\pi^*$ and n–$\pi^*$ transition, respectively. After dipping, the 330 nm peak significantly decreased and a new transition band appeared at bout 290 nm and a shoulder peak increased at about 810 nm.

Since PAANI is a linear molecule with long conjugated chain system, containing alternating phenol and nitrogen groups, can be a good electron donor and acceptor. The conjugation between the phenol groups and Pt(0) is possible. The structure of the

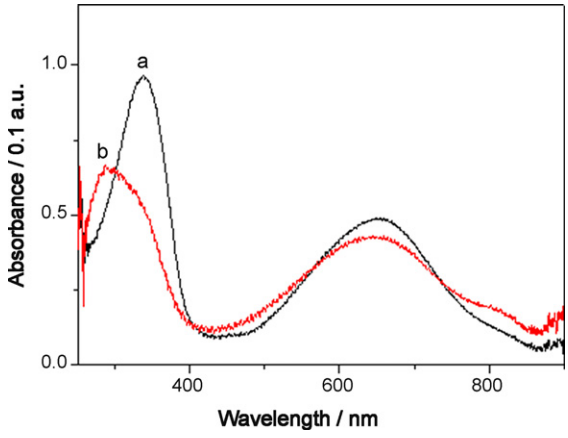


Fig. 5. UV–vis spectrum of PAANI (a) and after dipping in $H_2PtCl_6$ solution for 30 min (b) in DMSO.

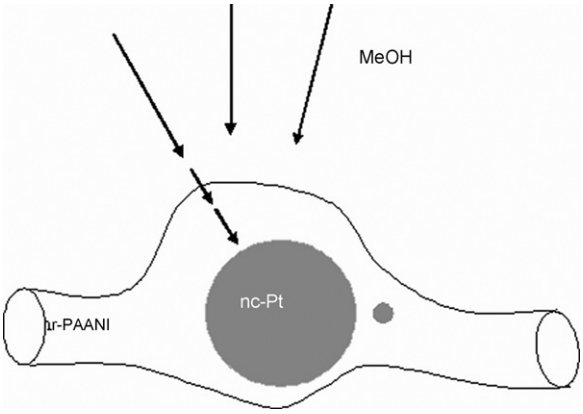


Scheme 2. Model for the nanocomposite nr-PAANI/nc-Pt, which consisted of nanorods (nr-PAANI) and embedded platinum nanocluster (nc-Pt). The arrows indicate the diffusion route of analyte: from the bulk solution, across the $H_2O$/PAANI interface, and to the surface of nc-Pt, respectively.

PAANI polymeric chain, as shown in Scheme 2, where the *x*:*y* is about 1:1, some *N*-substituted acetyl groups could be eliminated during polymerization [22]. It is more likely that the decrease of 330 nm bands and the appearance of 290 bands indicated the Pt(0), after full reduction, stabilizes the π orbital of the conjugated polymer because it can donate electron density to the polymer through its valance band. Hence, this interaction between the polymeric chains and the embedded Pt particles not only stabilize the nanostructures but also provide a modified Pt nanoelectrode arrays, which is an advantage for electrochemistry.

### 3.5. Electrocatalytic oxidation of methanol

Electrochemical oxidation of methanol was tested in 0.5 M $H_2SO_4$ solution, as shown in Fig. 6. The Pt/PAANI/GCE with 38 μg cm$^{-2}$ Pt loading gave three redox couples in the blank solution (curve a), a bell-shape oxidation peak of methanol appeared at 0.65 V in the presence of 0.5 M methanol (curve b), and bell-shape oxidation peak at 0.48 V appeared in the reverse scan. The peak at 0.48 V is associated with a removal of incompletely oxidized carbonaceous species generated from the methanol oxidation on the surface layer [31]

$$\text{Pt-(CO)}_{ad} + \text{Pt-(OH)}_{ad} \rightarrow \text{CO}_2 + \text{H}^+ + \text{e} + 2\text{Pt}.$$

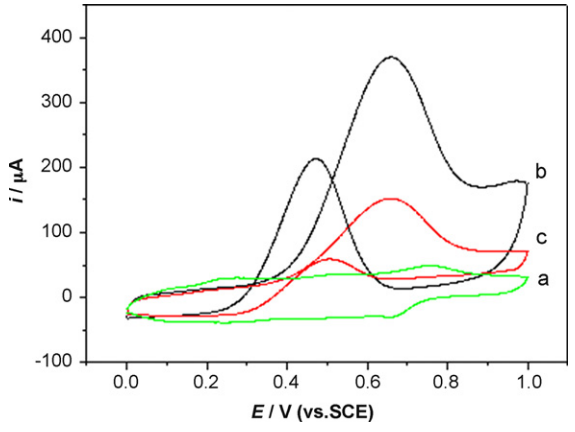


Fig. 6. CVs of Pt/PAANI/GCE with 38 μg cm$^{-2}$ Pt loading (a and b) and Pt/GCE with 41 μg cm$^{-2}$ Pt loading (c) in the absence (a) and presence of 0.5 M $CH_3OH$ (b and c). Scan rate: 10 mV s$^{-1}$.

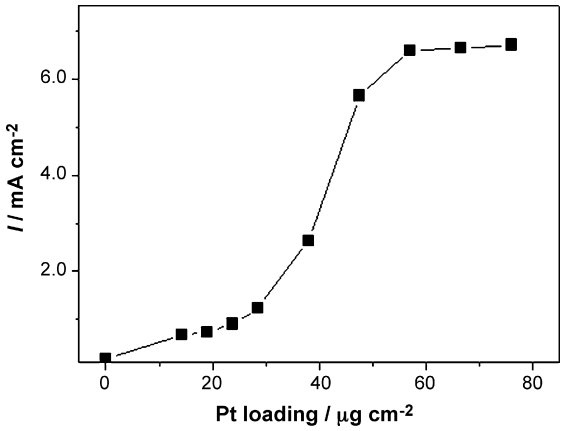


Fig. 7. Plot of $i_{pa}$ of 0.5 M methanol vs. Pt loading of Pt/PAANI/GCE.

For comparison, the CV at the Pt/GCE with similar Pt loadings is shown in curve c. The oxidation peak of methanol is also appeared at 0.65 V, however, with much smaller peak current. It is believed that the polymeric structures could prevent embedded nanoparticles from agglomerating and coalescing [19,32,33]. The 2.5-fold increase in peak current at the Pt/PAANI/GCE is possibly attributed to the dispersion of nc-Pt in the PAANI matrix, resulting in a significantly higher surface area thus causing an increase in the catalytic activity. The bell shape of the oxidation peak agrees well with the mode of surface confined or thin-layer limited waves. The peak current ($i_{pa}$) was proportional to the scan rate ($v$) for $2 < v < 20$ mV s$^{-1}$, and was a linear function of $v^{1/2}$ in the range of 50–600 mV s$^{-1}$, indicating a diffusion-controlled surface wave.

The interaction between the PAANI and methanol was examined by CV experiment. It was found that the PAANI/GCE did not catalyze the oxidation of methanol in the potential window, however, the three characteristic redox peaks of PAANI were diminished by an addition of methanol. The methanol molecules may be adsorbed into the nr-PAANI by hydrophobic interactions and reduced the conductivity of the nanorods.

The $i_{pa}$ at the Pt/PAANI/GCE versus the Pt loading was examined as shown in Fig. 7. The current density ($I$) was defined as the ratio of $i_{pa}$ divided by the formal surface area 0.126 cm$^{-2}$. As seen from the figure, $I$ increased to a plateau 6.3 mA cm$^{-2}$ for the Pt loadings became larger than 57 μg cm$^{-2}$. The mechanism for the saturation is complicated since it should be determined not only the kinetics of transportation, adsorption and reaction of methanol but also the generation and reaction of relevant species such as OH–, $(CO)_{ad}$, etc. However, the catalytic current efficiency, which could be defined as the ratio of the maximal sensitivity (6.3 mA cm$^{-2}$) divided by the Pt loading (57 μg cm$^{-2}$), is larger than that reported for a Pt-modified polyaniline electrodes [12].

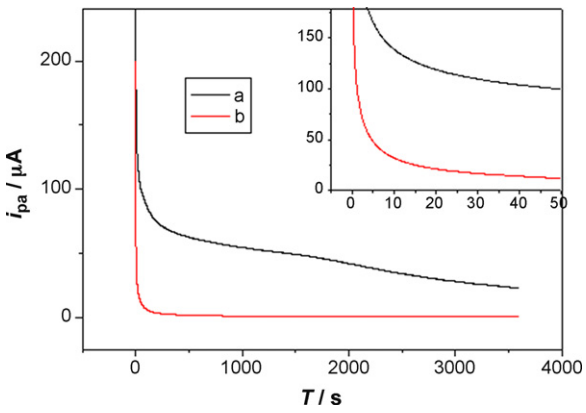


Fig. 8. Chronoamperometric curves of the Pt/PAANI/GCE (a) and the Pt/GCE (b) at 0.65 V in 0.5 M $CH_3OH$ solution (the inset is the plot at an enlarged time scale). Electrolyte: 0.5 M $H_2SO_4$.

Chronoamperometry was used to characterize the stability as shown in Fig. 8. The $i_{pa}$ at the Pt/PAANI/GCE (curve a) showed a relatively stable plateau during the first 1500 s at about 60 μA electrolysis current, and then the current was gradually decaying down to about 25 μA at 1 h. Comparatively, at the Pt/GCE, the current (curve b) was decaying very quickly down to 25 μA in about only 10 s as shown in the inset. Multi-cycle CV was also used for the examination. The $i_{pa}$ at the Pt/PAANI/GCE decreased gradually with increasing the cycle number in 0.5 M $H_2SO_4$ + 0.5 M $CH_3OH$. A 25.4% loss of $i_{pa}$ was observed at cycle number of 300. This is even more stable than a vapor deposited Pt nanoparticles modified electrodes [25].

The increased stability could be related to a reduction of the accumulation of poisonous species (such as $CO_{ad}$) on the surface of the Pt nanoparticles and stabilization of nanostructures by the PAANI coating environment. The adsorption ability of CO on the PAANI coated Pt surface may be less stable in comparison with that on a bare Pt.

Preliminary study showed that the Pt/PAANI/GCE has strong electrocatalytic activity toward oxidations of ethanol and formaldehyde, too. The CV parameters for catalytic oxidation of methanol, ethanol and formaldehyde at the Pt/PAANI/GCE in comparison with the Pt/GCE are summarized in Table 1. Based on the $E_{pa}$ values, the catalytic activity can be evaluated as in the order of $H_2CO$ > EtOH > MeOH at the Pt/PAANI/GCE, but MeOH > $H_2CO$ > EtOH at the Pt/GCE. The current sensitivity was in the order of $H_2CO \gg$ MeOH $\gg$ EtOH for both of these electrodes.

Table 1
CV data for electrocatalytic oxidation of methanol, ethanol and formaldehyde at different electrodes

| Substance | Pt/PAANI/GCE | | Pt/GCE | |
|---|---|---|---|---|
| | $E_{pa}$ (V) vs. SCE | $i_{pa}$ (mA cm$^{-2}$) | $E_{pa}$ (V) vs. SCE | $i_{pa}$ (mA cm$^{-2}$) |
| MeOH | 0.655 | 2.6 | 0.654 | 0.91 |
| EtOH | 0.639 | 0.76 | 0.688 | 0.37 |
| $H_2CO$ | 0.620 | 22.5 | 0.667 | 10.6 |

Scan rate, 10 mV s$^{-1}$; Pt loading, 38 μg cm$^{-2}$; $A$, 0.126 cm$^2$.

### 3.6. Synergic effect of the composite

At Pt/GCE, methanol should undergo dissociative–adsorption processes during the oxidation, generating carboxyl intermediates $(CH_xO)_{ad}$ ($x$ = 1–3) and $CO_{ad}$, which can be further oxidized to $CO_2$ by adsorbed oxygen containing species such as $OH_{ad}$ dissociated from adsorbed $H_2O$ [34]. Methanol should undergo the same reaction rote at the Pt/PAANI/GCE. However, the presence of the PAANI nanothickness coatings on nc-Pt surfaces, forming the composite nc-Pt/nr-PAANI, enhanced catalytic activity of Pt and reduced CO poisoning. The synergic effect of the nr-PAANI coating layers can be expressed as altering the solution/Pt interface into solution/PAANI/Pt interface.

Evidently, the Pt/PAANI/GCE has higher catalytic activity toward $H_2CO$ than methanol oxidation (Table 1), indicating that $H_2CO$, as an intermediate of methanol oxidation, could be oxidized at accelerated rates at the electrodes. This implies the rate determining step of the methanol oxidation may be different from that at regular Pt electrodes. Second, the significantly enhanced activity shown in the chronoamperometry (Fig. 8) evidently indicated much less poisoning accumulation at Pt surfaces was resulted at the Pt/PAANI/GCE. We suggest that the coated PAANI layers on Pt nanoparticles may reduce the adsorption strength of methanol and corresponding reaction intermediates. This is probable because the hydrophobic affinity of PAANI may result in dissolving and extracting methanol and reaction intermediates from Pt surfaces, and the donor–acceptor ability of PAANI is favorable for trapping, accumulating and transferring radicals, such as OH, H, to accelerate the reaction. Third, the Pt nanocluster structures were stabilized by the PAANI coating. The highly dispersed and stable 8.4 nm Pt nanoparticles provided large active surface for the oxidation.

## 4. Conclusions

We have prepared a novel nanorods 3D matrix of PAANI and a Pt nanocluster embedded PAANI nanorods composite at a glassy carbon electrodes by potential cycling. The composite modified electrode (Pt/PAANI/GCE) was used for catalytic oxidation of methanol in acidic solution. We have found that the Pt/PAANI/GCE has enhanced electocatalytic activity toward methanol oxidation and has significantly reduced poisoning effect. The findings suggest that the synergic effect of the nano-PAANI polymeric coating on Pt nanoclusters provides a nanothickness hydrophobic and conjugative environment for accumulating methanol, stabilizing the nanostructure, extracting intermediates and poisoning species.

## Acknowledgements

We gratefully acknowledge the financial support from the Specialized Research Fund for the Doctoral Program of Higher Education (No. 20040358021) and National Natural Science Foundation of China (No. 20575062).

## References


[1] R. Dillon, S. Srinivasan, A.S. Arico, V. Antonucci, J. Power Sources 127 (2004) 112.
[2] P.S. Kauranen, Acta Polytech. Scand.-Chem. Technol. Ser. (1996) 1.
[3] X.M. Ren, P. Zelenay, S. Thomas, J. Davey, S. Gottesfeld, J. Power Sources 86 (2000) 111.
[4] J. Leger, C. Lamy, Phys. Chem. 94 (1990) 1021.
[5] M. Gholamian, J. Sundaram, A.Q. Contractor, Langmuir 3 (1987) 741.
[6] B. Rajesh, K.R. Thampi, J.M. Bonard, H.J. Mathieu, N. Xanthopoulos, B. Viswanathan, Electrochem. Solid St. 7 (2004) A404.
[7] P. Sen, S. Laha, I.N. Basumallick, Bull. Electrochem. 20 (2004) 125.
[8] A.P. O'Mullane, S.E. Dale, J.V. Macpherson, P.R. Unwin, Chem. Commun. 10 (2004) 1606.
[9] J.H. Choi, Y.M. Kini, J.S. Lee, K.Y. Cho, H.Y. Jung, J.K. Park, I.S. Park, Y.E. Sung, Solid State Ionics 176 (2005) 3031.
[10] G. Wu, L. Li, J.H. Li, B.Q. Xu, J. Power Sources 155 (2005) 118.
[11] W.S. Li, J. Lu, J.H. Du, D.S. Lu, H.Y. Chen, H. Li, Y.M. Wu, Electrochem. Commun. 7 (2005) 406.
[12] L. Niu, Q.H. Li, F.H. Wei, S.X. Wu, P.P. Liu, X.L. Cao, J. Electroanal. Chem. 578 (2005) 331.
[13] H. Yang, T.H. Lu, K.H. Xue, S.G. Sun, G.Q. Lu, S.P. Chen, J. Electrochem. Soc. 144 (1997) 2302.
[14] I. Becerik, S. Suzer, F. Kadirgan, J. Electroanal. Chem. 476 (1999) 171.
[15] S. Moravcova, K. Bouzek, J. Electrochem. Soc. 152 (2005) A2080.
[16] M. Hepel, J. Electrochem. Soc. 145 (1998) 124.
[17] I. Becerik, F. Kadirgan, Synth. Met. 124 (2001) 379.
[18] S. Biallozor, A. Kupniewska, Bull. Electrochem. 20 (2004) 241.
[19] A.N. Golikand, S.M. Golabi, M.G. Maragheh, L. Irannejad, J. Power Sources 145 (2005) 116.
[20] L.Z. Zheng, S.G. Wu, X.Q. Lin, L. Nie, L. Rui, Analyst 126 (2001) 736.
[21] S.G. Wu, L.Z. Zheng, L. Rui, X.Q. Lin, Electroanalysis 13 (2001) 967.
[22] L.Z. Zheng, S.G. Wu, X.Q. Lin, L. Nie, L. Rui, Macromolecules 35 (2002) 6174.
[23] S.Q. Wang, L.P. Lu, X.Q. Lin, Electroanalysis 16 (2004) 1734.
[24] S.G. Wu, X.G. Han, Polym. Degrad. Stabil. 90 (2005) 535.
[25] Z.B. He, J.H. Chen, D.Y. Liu, H. Tang, W. Deng, Y.F. Kuang, Mater. Chem. Phys. 85 (2004) 396.
[26] J.M. Kinyanjui, N.R. Wijeratne, J. Hanks, D.W. Hatchett, Electrochim. Acta 51 (2006) 2825.
[27] D.W. Hatchett, R. Wijeratne, J.M. Kinyanjui, J. Electroanal. Chem. 593 (2006) 203.
[28] V. Radmilovic, H.A. Gasteiger, P.N. Ross, J. Catal. 154 (1995) 98.
[29] X.Q. Lin, Y.X. Li, Biosens. Bioelectron. 22 (2006) 253.
[30] A. Malinauskas, J. Malinauskiene, A. Ramanavicius, Nanotechnology 16 (2005) R51.
[31] R. Manoharanr, J.B. Goodenough, J. Mater. Chem. 2 (1992) 875.
[32] D. Profeti, P. Olivi, Electrochim. Acta 49 (2004) 4979.
[33] S.M. Golabi, A. Nozad, J. Electroanal. Chem. 521 (2002) 161.
[34] H. Laborde, J.M. Leger, C. Lamy, J. Appl. Electrochem. 24 (1994) 219.